

# F-Theory Grand Unification at the Colliders

Tianjun Li,<sup>1,2</sup> James A. Maxin,<sup>1</sup> and Dimitri V. Nanopoulos<sup>1,3,4</sup>

<sup>1</sup>*George P. and Cynthia W. Mitchell Institute for Fundamental Physics,  
Texas A&M University, College Station, TX 77843, USA*

<sup>2</sup>*Key Laboratory of Frontiers in Theoretical Physics, Institute of Theoretical Physics,  
Chinese Academy of Sciences, Beijing 100190, P. R. China*

<sup>3</sup>*Astroparticle Physics Group, Houston Advanced Research Center (HARC), Mitchell Campus, Woodlands, TX 77381, USA*

<sup>4</sup>*Academy of Athens, Division of Natural Sciences,  
28 Panepistimiou Avenue, Athens 10679, Greece*

We predict the exact gaugino mass relation near the electroweak scale at one loop for gravity mediated supersymmetry breaking in F-theory  $SU(5)$  and  $SO(10)$  models with  $U(1)_Y$  and  $U(1)_{B-L}$  fluxes, respectively. The gaugino mass relation introduced here differs from the typical gaugino mass relations studied thus far, and in general, should be preserved quite well at low energy. Therefore, these F-Theory models can be tested at the Large Hadron Collider and future International Linear Collider. We present two typical scenarios that satisfy all the latest experimental constraints and are consistent with the CDMS II experiment. In particular, the gaugino mass relation is indeed satisfied at two-loop level with only a very small deviation around the electroweak scale.

PACS numbers: 11.10.Kk, 11.25.Mj, 11.25.-w, 12.60.Jv

## INTRODUCTION

The great challenge of string phenomenology is constructing realistic string models which allow us to make unique predictions that can be tested at the Large Hadron Collider (LHC), future International Linear Collider (ILC), and other experiments. If these predictions are confirmed at future experiments, we will possess strong evidence to support that string theory is indeed the correct fundamental description of nature. To the present, string phenomenology has been primarily concentrated on heterotic  $E_8 \times E_8$  string theory and Type II string theories with D-branes, though unfortunately, this has not resulted in any unique prediction thus far.

The last two years have seen Grand Unified Theories (GUTs) constructed locally in F-theory, which can be considered as the strongly coupled formulation of ten-dimensional Type IIB string theory with a varying axion-dilaton field  $S$  [1–5]. In F-theory model building, the gauge fields reside on the observable seven-branes that wrap a del Pezzo  $n$  ( $dP_n$ ) surface for the extra four space dimensions, while the Standard Model (SM) fermions and Higgs fields are localized on the complex codimension one curves (two-dimensional real subspaces) in  $dP_n$ . Certainly, F-Theory model building and phenomenology have been studied extensively [6–13]. In contrast to D-brane model building [14], all the SM fermion Yukawa couplings can be obtained from the triple intersections of the SM fermion and Higgs curves. An exciting new feature is that  $SU(5)$  gauge symmetry can be broken down to the SM gauge symmetry by turning on  $U(1)_Y$  flux [3, 4, 12], and additionally, the  $SO(10)$  gauge symmetry can be broken down to the  $SU(5) \times U(1)_X$  and  $SU(3) \times SU(2)_L \times SU(2)_R \times U(1)_{B-L}$  gauge symmetries by turning on the  $U(1)_X$  and  $U(1)_{B-L}$  fluxes, respec-

tively [3, 4, 6, 7, 11, 12]. It is significant to note that realistic GUTs from F-theory can be constructed locally, hence, the next key question is whether a unique prediction can be made that can be tested at the LHC, ILC, and other future experiments.

To study the low energy phenomenology from F-theory GUTs, gauge mediated supersymmetry breaking was predominantly considered since the F-theory GUTs were constructed locally [9]. However, to construct realistic F-theory GUTs, we must embed these local GUTs into a globally consistent framework [10]. Consequently, here we study gravity mediated supersymmetry breaking. In F-theory  $SU(5)$  and  $SO(10)$  models where the gauge symmetries are broken down to the  $SU(3) \times SU(2)_L \times U(1)_Y$  and  $SU(3) \times SU(2)_L \times SU(2)_R \times U(1)_{B-L}$  gauge symmetries by turning on the  $U(1)_Y$  and  $U(1)_{B-L}$  fluxes, respectively, we obtain the exact gaugino mass relation (See Eq. (8) in the following) near the electroweak scale at one loop. These F-theory GUTs are constructed locally, so we do not know the Kähler potential for the SM fermions and Higgs fields. For this reason, we cannot calculate the supersymmetry breaking scalar masses and trilinear soft terms. Interestingly, our gaugino mass relation can be preserved very well at the low energy two-loop level if the scalar masses and trilinear soft terms are near the TeV scale. Using the indices for the gaugino mass relations [15, 16], we show that our gaugino mass relation is different from those that have been studied thus far [17]. Because the gaugino masses can be measured at LHC and ILC [18–20], these F-theory GUTs can be tested at the colliders. Note that the generic scalar masses and trilinear soft terms will not affect our prediction on the gaugino mass relation at low energy, so we assume a universal scalar mass  $m_0$  and universal trilinear soft term  $A_0$  for simplicity. Examining two typical

scenarios of gaugino masses, we present the viable parameter space which satisfies all the latest experimental constraints and is consistent with the CDMS II experiment [21]. In particular, the gaugino mass relation is in fact satisfied at two-loop level with only a very slight deviation at low energy. More detailed discussions will be presented elsewhere [22].

## GAUGINO MASS RELATION

In the F-theory GUTs, the GUT gauge symmetries on the observable seven-branes are broken by turning on the  $U(1)$  fluxes. Interestingly, these  $U(1)$  fluxes will give additional contribution to the gauge kinetic functions, which can be computed by dimensionally reducing the Chern-Simons action of the observable seven-branes wrapping on  $dP_n$

$$S_{\text{CS}} = \mu_7 \int_{dP_n \times \mathbb{R}^{3,1}} a \wedge \text{tr}(F^4). \quad (1)$$

For simplicity, we will assume that the heavy KK states and string states have masses above the GUT scale, which can be realized naturally in the global F-theory GUTs.

First, let us consider the  $SU(5)$  models [3, 4, 12]. Turning on the  $U(1)_Y$  flux, the gauge kinetic functions  $f_3$ ,  $f_2$  and  $f_1$  respectively for  $SU(3)_C$ ,  $SU(2)_L$  and  $U(1)_Y$  gauge symmetries at the string scale can be parametrized as follows [5, 8]

$$\begin{aligned} f_3 &= \tau + \frac{1}{2}\alpha S, \quad f_2 = \tau + \frac{1}{2}(\alpha + 2)S, \\ f_1 &= \tau + \frac{1}{2}\left(\alpha + \frac{6}{5}\right)S, \end{aligned} \quad (2)$$

where  $\tau$  is the original gauge kinetic function of  $SU(5)$ , the  $S$  terms arise from  $U(1)_Y$  flux contributions, and  $\alpha$  is a positive integer.

Second, let us consider the  $SO(10)$  models. If the  $SO(10)$  gauge symmetry is broken down to the flipped  $SU(5) \times U(1)_X$  gauge symmetry by turning on the  $U(1)_X$  flux [3, 4, 7, 11], we can show that the gauge kinetic functions for  $SU(5)$  and  $U(1)_X$  are exactly the same at the unification scale [11]. Interestingly, if we break the  $SO(10)$  gauge symmetry down to the  $SU(3) \times SU(2)_L \times SU(2)_R \times U(1)_{B-L}$  gauge symmetry by turning on the  $U(1)_{B-L}$  flux [6, 12], we can show that the gauge kinetic functions for the  $SU(3)_C$ ,  $U(1)_{B-L}$ ,  $SU(2)_L$ , and  $SU(2)_R$  gauge symmetries at the string scale are [12]

$$\begin{aligned} f_{SU(3)_C} &= f_{U(1)_{B-L}} = \tau + S, \\ f_{SU(2)_L} &= f_{SU(2)_R} = \tau, \end{aligned} \quad (3)$$

where  $\tau$  is the original gauge kinetic function of  $SO(10)$ , and the  $S$  term arises from  $U(1)_{B-L}$  flux contribution. We can break the  $SU(2)_R \times U(1)_{B-L}$  gauge symmetry

down to  $U(1)_Y$  at the string scale by the Higgs mechanism. As a consequence, we obtain the gauge kinetic function for  $U(1)_Y$  [12]

$$f_{U(1)_Y} = \frac{3}{5}f_{SU(2)_R} + \frac{2}{5}f_{U(1)_{B-L}} = \tau + \frac{2}{5}S. \quad (4)$$

Now, let us study gravity mediated supersymmetry breaking. We can show that the gaugino mass relation in the  $SO(10)$  models with  $U(1)_{B-L}$  flux is the same as that in the  $SU(5)$  models with  $U(1)_Y$  flux. Henceforth, we only consider the  $SU(5)$  models with  $U(1)_Y$  flux here. Supposing supersymmetry is broken by the F-terms of  $\tau$  and  $S$ , we can parametrize  $F^\tau$  and  $F^S$  as follows

$$F^\tau = M'_{3/2}(\tau + \bar{\tau}) \cos \theta, \quad F^S = M'_{3/2}(S + \bar{S}) \sin \theta, \quad (5)$$

where  $M'_{3/2}$  is the gravitino mass if supersymmetry is only broken by the F-terms of  $\tau$  and  $S$ . Then, the gaugino masses  $M_3$ ,  $M_2$ , and  $M_1$  respectively for  $SU(3)_C$ ,  $SU(2)_L$ , and  $U(1)_Y$  at the GUT scale are

$$\begin{aligned} M_3 &= \frac{\cos \theta + \alpha x \sin \theta}{1 + \alpha x} M'_{3/2}, \\ M_2 &= \frac{\cos \theta + (\alpha + 2)x \sin \theta}{1 + (\alpha + 2)x} M'_{3/2}, \\ M_1 &= \frac{5 \cos \theta + (5\alpha + 6)x \sin \theta}{5 + (5\alpha + 6)x} M'_{3/2}, \end{aligned} \quad (6)$$

where  $x$  is defined as

$$x = \frac{S + \bar{S}}{2(\tau + \bar{\tau})}. \quad (7)$$

Using the one-loop renormalization group equations (RGEs), we obtain the gaugino mass relation around the electroweak scale

$$\frac{M_1}{\alpha_1} - \frac{M_3}{\alpha_3} = \frac{3}{5} \left( \frac{M_2}{\alpha_2} - \frac{M_3}{\alpha_3} \right), \quad (8)$$

where  $\alpha_3$ ,  $\alpha_2$ , and  $\alpha_1$  are the gauge couplings for the  $SU(3)_C$ ,  $SU(2)_L$ , and  $U(1)_Y$  gauge symmetries, respectively. Following Refs. [15, 16], we define the index  $k$  for the gaugino mass relation as follows

$$k = \frac{M_2 \alpha_2^{-1} - M_3 \alpha_3^{-1}}{M_1 \alpha_1^{-1} - M_3 \alpha_3^{-1}}. \quad (9)$$

Thus, in the F-theory  $SU(5)$  and  $SO(10)$  models respectively with  $U(1)_Y$  and  $U(1)_{B-L}$  fluxes, we obtain that the index for gaugino mass relation is  $5/3$ , *i.e.*,  $k = 5/3$ . Moreover, in the minimal supersymmetric Standard Model with anomaly mediation and mirage mediation [17], we can show that the index for gaugino mass relation is  $5/12$ , *i.e.*,  $k = 5/12$  [16]. Thus, we emphasize that our gaugino mass relation is different from those in simple anomaly mediation and mirage mediation [17]. Furthermore, the index for gaugino mass relation in the

minimal Supergravity (mSUGRA) [17] is not well defined but can be formally written as  $0/0$ , *i.e.*,  $k = 0/0$  [15]. So the gaugino mass relation in mSUGRA satisfies the above gaugino mass relation in Eq. (8). However, if  $2(M_1\alpha_1^{-1} - M_3\alpha_3^{-1})/(M_1\alpha_1^{-1} + M_3\alpha_3^{-1})$  is not very small, our gaugino mass relation can definitely be distinguished from that of mSUGRA. Moreover, the gaugino masses can be measured at the LHC and ILC [18–20]. Therefore, these F-theory GUTs can be tested at the LHC and ILC, and may be distinguished from the mSUGRA, simple anomaly mediation and mirage mediation [17].

To test the gaugino mass relation close to the electroweak scale, we define a parameter  $\eta$  as follows

$$\eta = \frac{5(M_1\alpha_1^{-1} - M_3\alpha_3^{-1})}{3(M_2\alpha_2^{-1} - M_3\alpha_3^{-1})}. \quad (10)$$

Notice  $\eta$  is exactly one at the GUT scale. In addition,  $\eta$  is one around the electroweak scale from one-loop RGE running, yet  $\eta$  may deviate slightly from one as a result of two-loop RGE running.

For simplicity, we assume that  $x$  is small in this work, and then we have approximate gauge coupling unification at the GUT scale, allowing us to use well-established public codes for computations. For gaugino masses, we consider two typical scenarios

(I) We consider the dilaton dominated scenario, *i.e.*,  $\theta = \pi/2$ . The gaugino masses at the GUT scale are

$$\begin{aligned} M_3 &\simeq \alpha M_{1/2}, \quad M_2 \simeq (\alpha + 2) M_{1/2}, \\ M_1 &\simeq \left(\alpha + \frac{6}{5}\right) M_{1/2}, \end{aligned} \quad (11)$$

where  $M_{1/2}$  is a mass parameter. In our numerical calculations, we will choose  $\alpha = 3$ .

(II) We consider the scenario where  $\cos\theta$  is on the order of  $x\sin\theta$ . Assuming  $\cos\theta > 0$  and  $\sin\theta < 0$ , we parametrize  $\cos\theta$  as follows

$$\cos\theta = -\gamma x \sin\theta, \quad (12)$$

where  $\gamma$  is a positive real number. Thus, we obtain the gaugino masses at the GUT scale

$$\begin{aligned} M_3 &\simeq (\gamma - \alpha) M_{1/2}, \quad M_2 \simeq (\gamma - \alpha - 2) M_{1/2}, \\ M_1 &\simeq \left(\gamma - \alpha - \frac{6}{5}\right) M_{1/2}. \end{aligned} \quad (13)$$

In our numerical calculations, we choose  $(\gamma - \alpha) = 5$ . In summary, we have  $M_3 < M_1 < M_2$  in scenario I and  $M_2 < M_1 < M_3$  in scenario II.

## LOW ENERGY SUPERSYMMETRY PHENOMENOLOGY

We take  $\mu > 0$ , so we have four free parameters in our models:  $M_{1/2}$ ,  $m_0$ ,  $A_0$ , and  $\tan\beta$ , where  $\tan\beta$  is the ratio of the Higgs vacuum expectation values. The soft supersymmetry breaking terms are input into `MicrOMEGAs`

2.0.7 [23] using `SuSpect` 2.34 [24] as a front end to run the soft terms down to the electroweak scale via RGEs and then to calculate the corresponding neutralino relic density. We use a top quark mass of  $m_t = 173.1$  GeV [25]. The direct detection cross-sections are calculated using `MicrOMEGAs` 2.1 [26]. We employ the following experimental constraints: (1) The WMAP  $2\sigma$  measurements of the cold dark matter density [27],  $0.095 \leq \Omega_\chi \leq 0.129$ . Also, we allow  $\Omega_\chi$  to be larger than the upper bound due to a possible  $\mathcal{O}(10)$  dilution factor [28] and to be smaller than the lower bound due to multicomponent dark matter. (2) The experimental limits on the Flavor Changing Neutral Current (FCNC) process,  $b \rightarrow s\gamma$ . The results from the Heavy Flavor Averaging Group (HFAG) [29], in addition to the BABAR, Belle, and CLEO results, are:  $Br(b \rightarrow s\gamma) = (355 \pm 24_{-10}^{+9} \pm 3) \times 10^{-6}$ . There is also a more recent estimate [30] of  $Br(b \rightarrow s\gamma) = (3.15 \pm 0.23) \times 10^{-4}$ . For our analysis, we use the limits  $2.86 \times 10^{-4} \leq Br(b \rightarrow s\gamma) \leq 4.18 \times 10^{-4}$ , where experimental and theoretical errors are added in quadrature. (3) The anomalous magnetic moment of the muon,  $g_\mu - 2$ . For this analysis we use the  $2\sigma$  level boundaries,  $11 \times 10^{-10} < \Delta a_\mu < 44 \times 10^{-10}$  [31]. (4) The process  $B_s^0 \rightarrow \mu^+\mu^-$  where the decay has a  $\tan^6\beta$  dependence. We take the upper bound to be  $Br(B_s^0 \rightarrow \mu^+\mu^-) < 5.8 \times 10^{-8}$  [32]. (5) The LEP limit on the lightest CP-even Higgs boson mass,  $m_h \geq 114$  GeV [33].

For scenario I, we commence with  $m_0$ ,  $A_0$ , and  $\tan\beta$  as free parameters, however, a comprehensive scan uncovers  $A_0 = m_0$  as the most phenomenologically favored. As shown in Fig. 1, the experimentally allowed parameter space for the Scenario I with  $\alpha = 3$ ,  $\beta = 2$ , and  $\tan\beta = 51$  after applying all these constraints consists of small  $M_{1/2}$  and large  $m_0$ . We choose a point within the narrow region that satisfies the WMAP relic density as our benchmark point for analysis. See table I for the supersymmetric particle (sparticle) and Higgs spectrum. In fact, with a relic density of  $\Omega_\chi = 0.1156$ , this benchmark point additionally satisfies the very constrained WMAP 5-year results [27]. For constant  $m_0 = A_0 = 740$  GeV, we find  $\tan\beta = 25$ -52 for  $0 \leq \Omega_\chi \lesssim 1.1$ , in contrast to  $\tan\beta = 41$  and  $\tan\beta = 51$ -52 for the WMAP region. In mSUGRA, the focus point region consists of large  $m_0$  where the WMAP observed relic density can be satisfied with a large Higgsino component in the lightest supersymmetric particle (LSP) neutralino due to a small  $|\mu|$ . However, even though  $m_0$  is reasonably large in comparison to  $M_{1/2}$  for this benchmark point, here the LSP is 98% bino. The WIMP-nucleon direct-detection cross-sections  $\sigma_{SI}$  depicted in Fig. 2 underscore the fact that the case of  $\alpha = 3$ ,  $\beta = 2$ , and  $\tan\beta = 51$  produces WIMPs with  $\sigma_{SI}$  just beneath the CDMS II [21] upper limit, with our benchmark point at  $\sigma_{SI} = 6.15 \times 10^{-8}$  pb and  $m_{\tilde{\chi}_1^0} = 316$  GeV. The constraints from previous ZEPLIN [34], XENON [35], and CDMS [36] experiments are also delineated on the plot.

TABLE I: Supersymmetric particle (sparticle) and Higgs spectrum for a Scenario I,  $\alpha = 3$ ,  $\beta = 2$  benchmark point with  $\sigma_{SI} = 6.15 \times 10^{-8}$  pb. Here,  $\tan\beta = 51$  and  $\Omega_\chi = 0.1156$ . The GUT scale mass parameters for this point are (in GeV)  $M_{1/2} = 180$ ,  $M_3 = 540$ ,  $M_2 = 900$ ,  $M_1 = 756$ ,  $m_0 = A_0 = 740$ .

$\tilde{\chi}_1^0$	316	$\tilde{\chi}_1^\pm$	473	$\tilde{e}_R$	790	$\tilde{t}_1$	973	$\tilde{u}_R$	1302	$m_h$	115.4
$\tilde{\chi}_2^0$	477	$\tilde{\chi}_2^\pm$	743	$\tilde{e}_L$	946	$\tilde{t}_2$	1201	$\tilde{u}_L$	1402	$m_A$	465
$\tilde{\chi}_3^0$	487	$\tilde{\nu}_{e/\mu}$	942	$\tilde{\tau}_1$	489	$\tilde{b}_1$	1103	$\tilde{d}_R$	1294	$m_{H^\pm}$	473
$\tilde{\chi}_4^0$	743	$\tilde{\nu}_\tau$	837	$\tilde{\tau}_2$	843	$\tilde{b}_2$	1195	$\tilde{d}_L$	1404	$\tilde{g}$	1263

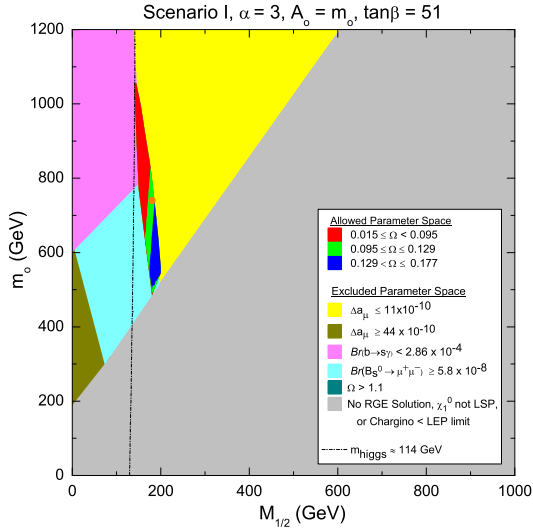


FIG. 1: Experimentally allowed parameter space for Scenario I,  $\alpha = 3$ ,  $\beta = 2$ ,  $A_0 = m_0$ ,  $\tan\beta = 51$ . The benchmark point detailed in Table I is annotated on the plot by the orange point.

The values of  $M_1$ ,  $M_2$ ,  $M_3$ ,  $\alpha_1$ ,  $\alpha_2$  and  $\alpha_3$  at electroweak-symmetry breaking (EWSB) are used to compute  $\eta$  in Eq. (10), and we find the deviation of  $\eta$  from one is very small, or on the order of 1.2% - 1.6%, as expected. The small deviation from one for  $\alpha = 3$ ,  $\beta = 2$ , and  $\tan\beta = 51$  is clearly shown in Fig. 3, thus, the gaugino mass relation in Eq. (8) can be tested at the LHC and ILC since the two-loop corrections are indeed very small.

The five lightest sparticles for the  $\alpha = 3$ ,  $\beta = 2$ , and  $\tan\beta = 51$  benchmark point, including the heavy Higgs, are  $\tilde{\chi}_1^0 < A < H^\pm < \tilde{\chi}_1^\pm < \tilde{\chi}_2^0$ . The productions of squarks  $\tilde{q}$  and gluino  $\tilde{g}$  have the largest differential cross-sections at LHC. The squark in the first two families will decay dominantly into the gluino  $\tilde{g}$  and the corresponding quark, and the gluino  $\tilde{g}$  decay will mainly produce either the sbottom  $\tilde{b}$  and bottom quark  $b$  or the stop  $\tilde{t}$  and top quark  $t$ . The  $\tilde{b}$  and  $\tilde{t}$  decay to the top quark  $t$ , bottom quark  $b$ , neutralino, and chargino. Additionally, we will get  $b$  quark from  $\tilde{\chi}_2^0$  through light Higgs in the process  $\tilde{\chi}_2^0 \rightarrow h_0 \tilde{\chi}_1^0$  with a branching ratio of 93%. These

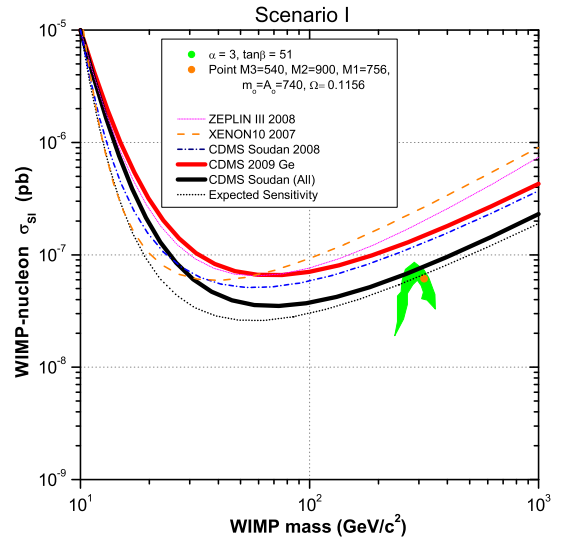


FIG. 2: Spin-independent WIMP-nucleon cross-sections for Scenario I,  $\alpha = 3$ ,  $\beta = 2$ ,  $A_0 = m_0$ ,  $\tan\beta = 51$ . The green shaded region satisfies all experimental constraints. The point detailed in Table I is annotated on the plot by the orange point.

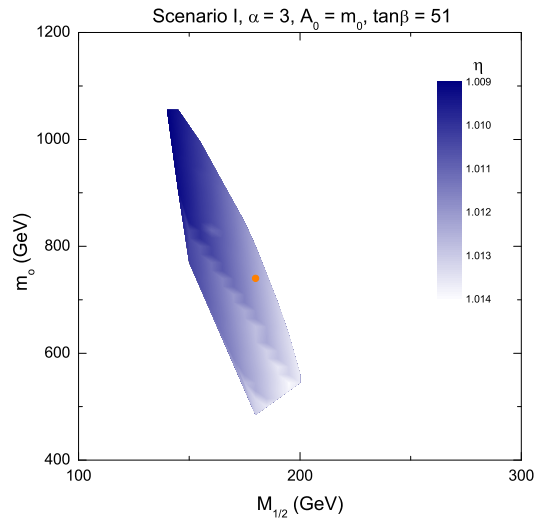


FIG. 3: Plot of  $\eta$  for Scenario I,  $\alpha = 3$ ,  $\beta = 2$ ,  $A_0 = m_0$ ,  $\tan\beta = 51$ . The shaded regions satisfy all experimental constraints. The point detailed in Table I is annotated on the plot by the orange point.

light Higgs will in turn decay to  $b\bar{b}$  with a 73% branching ratio. Leptons and hadronic jets will result from the decay  $\tilde{\chi}_1^\pm \rightarrow W^\pm \tilde{\chi}_1^0$ , where this is the only kinematically allowed  $\tilde{\chi}_1^\pm$  process. Due to the less massive nature of the heavy Higgs particles, the  $q\bar{q}$  reaction will provide some neutral heavy Higgs field  $A$  that will decay to  $b\bar{b}$  pair 87% of the time, while the heavy charged Higgs field  $H^\pm$  will produce  $\bar{b}t$  or  $b\bar{t}$  pair 84% of the time, with  $t \rightarrow W^+ b$ . Thus, this benchmark point will produce mainly light

Higgs field  $h_0$ ,  $b$  quark, and  $W$  boson at LHC.

In addition to the viable parameter space of Scenario I, Scenario II can also generate a well constrained region at the relic densities we consider here. Exhibited in Fig. 4 is the experimentally allowed region of small  $m_0$  and  $M_{1/2}$  for Scenario I with  $\gamma - \alpha = 5$ ,  $\beta = 2$ ,  $A_0 = m_0$ , and  $\tan\beta = 27$ . Choosing a benchmark point with  $M_{1/2} = 110$  GeV and  $m_0 = A_0 = 190$  GeV, we present the sparticle and Higgs spectrum in Table II. Because the small mass difference of 10 GeV between the LSP neutralino  $\tilde{\chi}_1^0$  and the next to the lightest supersymmetric particle (NLSP)  $\tilde{\tau}_1^\pm$ , the LSP neutralino in the early Universe can annihilate with stau and then we can obtain the correct dark matter density, similar to the stau-neutralino coannihilation region in mSUGRA. Moreover, the LSP for this point is 99.7% bino. Considering a constant  $m_0 = A_0 = 190$  GeV, we discover  $\tan\beta = 8-59$  for  $0 \leq \Omega_\chi \lesssim 1.1$ , but only  $\tan\beta = 18-27$  for the WMAP region. This Scenario II benchmark point possesses a  $\sigma_{SI} = 2.03 \times 10^{-8}$  pb at  $m_{\tilde{\chi}_1^0} = 170$  GeV, near the CDMSII upper limit. Furthermore, a calculation of  $\eta$  in Eq. (10) for this Scenario II benchmark point yields comparable results to the Scenario I benchmark point, namely only a very small deviation from one, on the order of 1.5% to 3.5%, as depicted in Fig. 6, corroborating the delineation of  $\eta$  in Fig. 3 and its testability. A close examination of this benchmark point reveals  $\tilde{\chi}_2^0 \rightarrow \tilde{\tau}_1^\mp \tau^\pm \rightarrow \tau^\mp \tau^\pm \tilde{\chi}_1^0$  as the dominant decay, therefore, we would expect opposite sign tau pair to be characteristic at the LHC.

TABLE II: Sparticle and Higgs spectrum for a Scenario II,  $\gamma - \alpha = 5$ ,  $\beta = 2$  benchmark point with  $\sigma_{SI} = 2.03 \times 10^{-8}$  pb. Here,  $\tan\beta = 27$  and  $\Omega_\chi = 0.107$ . The GUT scale mass parameters for this point are (in GeV)  $M_{1/2} = 110$ ,  $M_3 = 550$ ,  $M_2 = 330$ ,  $M_1 = 418$ ,  $m_0 = A_0 = 190$ .

$\tilde{\chi}_1^0$	170	$\tilde{\chi}_1^\pm$	256	$\tilde{e}_R$	247	$\tilde{t}_1$	922	$\tilde{u}_R$	1117	$m_h$	115.7
$\tilde{\chi}_2^0$	256	$\tilde{\chi}_2^\pm$	687	$\tilde{e}_L$	293	$\tilde{t}_2$	1080	$\tilde{u}_L$	1126	$m_A$	661
$\tilde{\chi}_3^0$	681	$\tilde{\nu}_{e/\mu}$	283	$\tilde{\tau}_1$	180	$\tilde{b}_1$	1033	$\tilde{d}_R$	1115	$m_{H^\pm}$	666
$\tilde{\chi}_4^0$	686	$\tilde{\nu}_\tau$	276	$\tilde{\tau}_2$	321	$\tilde{b}_2$	1095	$\tilde{d}_L$	1129	$\tilde{g}$	1257

Let us comment on the phenomenological differences between our models and the other supersymmetry breaking mediation models. Because our gaugino mass relation is different from those in the mSUGRA, simple anomaly mediation and mirage mediation, our gaugino mass ratio  $M_1 : M_2 : M_3$  at the low energy are different from those in the mSUGRA, simple anomaly mediation and mirage mediation. And then the neutralino masses, chargino masses and gluino mass will be different as well, which will affect the dark matter density and the productions and decays of the supersymmetric particles at the LHC.

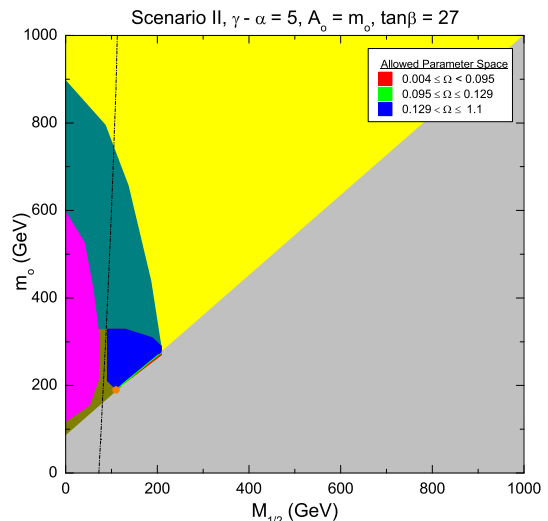


FIG. 4: Experimentally allowed parameter space for Scenario II,  $\gamma - \alpha = 5$ ,  $\beta = 2$ ,  $A_0 = m_0$ ,  $\tan\beta = 27$ . The benchmark point detailed in Table II is annotated on the plot by the orange point. Identification of the excluded regions is shown in the chart legend in Fig. 1.

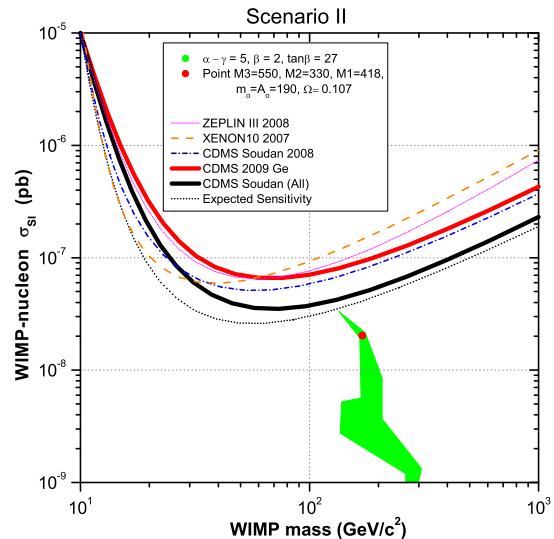


FIG. 5: Spin-independent WIMP-nucleon cross-sections for Scenario II,  $\gamma - \alpha = 5$ ,  $\beta = 2$ ,  $A_0 = m_0$ ,  $\tan\beta = 27$ . The green shaded region satisfies all experimental constraints. The point detailed in Table II is annotated on the plot by the orange point.

## CONCLUSION

We considered gravity mediated supersymmetry breaking and derived the exact gaugino mass relation at one loop near the electroweak scale in the F-theory  $SU(5)$  and  $SO(10)$  models with  $U(1)_Y$  and  $U(1)_{B-L}$  fluxes, respectively. The gaugino mass relation presented in this work differs from the typical gaugino mass relations that

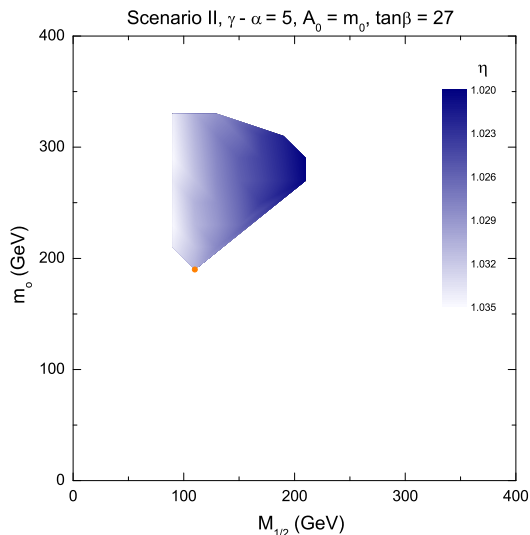


FIG. 6: Plot of  $\eta$  for Scenario II,  $\gamma - \alpha = 5$ ,  $\beta = 2$ ,  $A_0 = m_0$ ,  $\tan\beta = 27$ . The shaded regions satisfy all experimental constraints. The point detailed in Table II is annotated on the plot by the orange point.

have been studied in the past, and should be preserved pretty well at low energy in general. Thus, these F-theory GUTs can be tested at the LHC and forthcoming ILC. We exhibited two concrete scenarios that satisfy all the latest experimental constraints and are consistent with the CDMS II experiment. Most importantly, the gaugino mass relation is indeed satisfied at two-loop level with only a very small deviation.

### Acknowledgments

This research was supported in part by the DOE grant DE-FG03-95-Er-40917 (TL and DVN), by the Natural Science Foundation of China under grant numbers 10821504 and 11075194 (TL), and by the Mitchell-Heep Chair in High Energy Physics (JM).

---

[1] C. Vafa, Nucl. Phys. B **469**, 403 (1996).  
 [2] R. Donagi and M. Wijnholt, arXiv:0802.2969 [hep-th].  
 [3] C. Beasley, J. J. Heckman and C. Vafa, JHEP **0901**, 058 (2009).  
 [4] C. Beasley, J. J. Heckman and C. Vafa, JHEP **0901**, 059 (2009).  
 [5] R. Donagi and M. Wijnholt, arXiv:0808.2223 [hep-th].  
 [6] A. Font and L. E. Ibanez, JHEP **0902**, 016 (2009).  
 [7] J. Jiang, T. Li, D. V. Nanopoulos and D. Xie, Phys. Lett. B **677**, 322 (2009).  
 [8] R. Blumenhagen, Phys. Rev. Lett. **102**, 071601 (2009).

[9] J. J. Heckman, G. L. Kane, J. Shao and C. Vafa, JHEP **0910**, 039 (2009); J. J. Heckman, J. Shao and C. Vafa, arXiv:1001.4084 [hep-ph].  
 [10] R. Donagi and M. Wijnholt, arXiv:0904.1218 [hep-th]; J. Marsano, N. Saulina and S. Schafer-Nameki, JHEP **0908**, 046 (2009); arXiv:0912.0272 [hep-th]; T. W. Grimm, S. Krause and T. Weigand, arXiv:0912.3524 [hep-th].  
 [11] J. Jiang, T. Li, D. V. Nanopoulos and D. Xie, arXiv:0905.3394 [hep-th].  
 [12] T. Li, arXiv:0905.4563 [hep-th].  
 [13] T. Li, D. V. Nanopoulos and J. W. Walker, arXiv:0910.0860 [hep-ph].  
 [14] D. Berenstein, arXiv:hep-th/0603103.  
 [15] T. Li and D. V. Nanopoulos, Phys. Lett. B **692**, 121 (2010).  
 [16] T. Li and D. V. Nanopoulos, arXiv:1005.3798 [hep-ph].  
 [17] K. Choi and H. P. Nilles, JHEP **0704**, 006 (2007), and references therein.  
 [18] W. S. Cho, K. Choi, Y. G. Kim and C. B. Park, Phys. Rev. Lett. **100**, 171801 (2008); M. M. Nojiri, Y. Shimizu, S. Okada and K. Kawagoe, JHEP **0806**, 035 (2008).  
 [19] V. D. Barger, T. Han, T. Li and T. Plehn, Phys. Lett. B **475**, 342 (2000).  
 [20] B. Altunkaynak, P. Grajek, M. Holmes, G. Kane and B. D. Nelson, JHEP **0904**, 114 (2009).  
 [21] Z. Ahmed *et al.* [The CDMS-II Collaboration], arXiv:0912.3592 [astro-ph.CO].  
 [22] T. Li, J. A. Maxin, D. V. Nanopoulos, in preparation.  
 [23] G. Belanger, F. Boudjema, A. Pukhov and A. Semenov, Comput. Phys. Commun. **176**, 367 (2007); Comput. Phys. Commun. **174**, 577 (2006); Comput. Phys. Commun. **149**, 103 (2002).  
 [24] A. Djouadi, J. L. Kneur and G. Moultaka, Comput. Phys. Commun. **176**, 426 (2007).  
 [25] [Tevatron Electroweak Working Group and CDF Collaboration and D0 Collab], arXiv:0903.2503 [hep-ex].  
 [26] G. Belanger, F. Boudjema, A. Pukhov and A. Semenov, Comput. Phys. Commun. **180**, 747 (2009).  
 [27] D. N. Spergel *et al.* [WMAP Collaboration], Astrophys. J. Suppl. **148**, 175 (2003); Astrophys. J. Suppl. **170**, 377 (2007).  
 [28] N. E. Mavromatos and D. V. Nanopoulos, AIP Conf. Proc. **1166**, 26 (2009), and references therein.  
 [29] E. Barberio *et al.* [Heavy Flavor Averaging Group (HFAG) Collaboration], [arXiv:0704.3575 [hep-ex]].  
 [30] M. Misiak *et al.*, Phys. Rev. Lett. **98**, 022002 (2007).  
 [31] G. W. Bennett *et al.* [Muon g-2 Collaboration], Phys. Rev. Lett. **92**, 161802 (2004).  
 [32] T. Aaltonen *et al.* [CDF Collaboration], Phys. Rev. Lett. **100**, 101802 (2008).  
 [33] R. Barate *et al.* [LEP Working Group for Higgs boson searches and ALEPH Collaboration], Phys. Lett. B **565**, 61 (2003); W. M. Yao *et al.* (Particle Data Group), J. Phys. G **33**, 1 (2006).  
 [34] V. N. Lebedenko *et al.*, Phys. Rev. D **80**, 052010 (2009).  
 [35] J. Angle *et al.* [XENON Collaboration], Phys. Rev. Lett. **100**, 021303 (2008).  
 [36] Z. Ahmed *et al.* [CDMS Collaboration], Phys. Rev. Lett. **102**, 011301 (2009).